Force Design of Tensegrity Structures by Enumeration of Vertices of Feasible Region

M. Ohsaki [a,*] J.Y. Zhang [a] Y. Ohishi [b]

[a] *Dept. of Architecture & Architectural Engineering, Kyoto University, Japan*

[b] *Computer Engineering & Consulting, Ltd., 5–1–11, Higashihara, Zama, Kanagawa 228–8567, Japan*

Abstract

An optimization approach is presented for force design of tensegrity structures by enumeration of the vertices of the feasible region of the prestresses, which is defined as the linear combinations of the coefficients of the self-equilibrium force vectors. The unilateral properties of the stresses in cables and struts are taken into consideration. In order to design the stiffest structure against uncertain external loads as well as specific external loads, a multiobjective optimization problem is formulated for simultaneous maximization of the lowest eigenvalue of the tangent stiffness matrix and minimization of the compliance against a specified set of external loads. In the numerical example, Pareto optimal solutions are found by enumerating the vertices of the feasible region of prestresses of a tensegrity grid, and the monotonicity properties of the objective functions are investigated.

Key words: Tensegrity, Force design, Self-equilibrium force, Multiobjective programming, Vertex enumeration

1 Introduction

Distribution of member forces at the self-equilibrium state; i.e., prestresses introduced into the members, has great influence on stiffness and stability of tensegrity structures. Hence, for the structures consisting of several independent modes of prestress, the stiffness against external loads is desirable to be maximized by optimization of the coefficients of the prestress modes, since the distribution of member forces is defined as the linear combination of these modes. The process of determination of member forces for the structure with given shape is called *force design*. The purpose of this study is to present an approach to force design of tensegrity structures. A technique for enumerating vertices of a polyhedron defined by linear equalities and inequalities are successfully utilized to enumerate the vertices of the feasible region of the coefficients of the independent prestress modes.

In the process of force design, the prestresses should be assigned considering the

* Kyoto University, Kyoto-Daigaku Katsura, Nishikyo, Kyoto 615-8540, Japan.
E-mail: ohsaki@archi.kyoto-u.ac.jp

stress unilateral property of the members; i.e., the tensegrity structure consists of cables and struts that can only transmit tensile and compressive forces, respectively. In some special cases, e.g., the tensegrity grid used as example structure in Section 5, a tensegrity structure may have some bars, which carry no prestress in the self-equilibrium state.

By the rigorous definition, a tensegrity structure is free-standing without any support, and the struts are connected by continuous cables and do not contact with each other [1,2]. Since the members carry self-equilibrium forces, every node should be balanced by these member forces at the self-equilibrium state. Furthermore, due to the existence of infinitesimal mechanisms, tensegrity structures are usually unstable in the unstressed state, and the mechanisms are stabilized by the prestresses in the members [3]. Therefore, the shapes and forces of tensegrity structures are highly interdependent. These distinct properties of tensegrity structures compared with conventional bar-joint structures lead to difficulties in the determination of the self-equilibrium shapes and distribution of prestresses so that the structure is appropriately stabilized.

The process of determining shapes and forces of tensegrity structures is called *form-finding*. There have been many excellent methods proposed for this process, e.g., see the review paper [4]. In most of the existing methods, the shape and member forces of the structure are to be determined simultaneously to discover novel shapes in view of aesthetic and mechanical properties. However, few researches have been carried out for determination of the force distribution to appropriately stabilize the structure with specified shape considering stress unilateral properties of the cables and struts.

Since tensegrity structures usually have several independent modes of member forces in the self-equilibrium state, the member forces are defined as the linear combination of these force modes. The authors presented an approach to force design of the structures with multiple independent force modes by solving a bi-objective optimization problem for maximizing the stiffness of the structure as well as minimizing the deviation of the forces from the specified values [5]. Since positive definiteness of the geometrical stiffness matrix with respect to the infinitesimal mechanisms, also called reduced stiffness matrix, is the necessary condition for the stability of tensegrity structures as discussed in [6], the members of the structure were assumed to have infinite stiffness so that the structure can deform only in the directions of the mechanisms.

In this paper, we incorporate practical situation that the members of the structure have finite stiffnesses. The eigenvalues of the tangent stiffness matrix and the external work against specified external loads, called compliance, are considered as two performance measures representing the stiffness of the structure. The constraints are given for member forces so that the cables and struts can transmit only tensile and compressive forces, respectively. Moreover, the upper and lower bounds are given for the member forces so that the absolute values of the stresses are moderately small. These bound constraints are expressed as linear inequality constraints with respect to the coefficients of the independent modes of the self-equilibrium forces. Therefore, the feasible, or admissible, coefficients satisfying all the constraints form a convex region. The monotonicity properties of the two performance measures with respect to the member forces are discussed. The compromise solutions called Pareto

optimal solutions are found by the enumeration of the vertices of the convex feasible region defined by linear inequalities. The effectiveness of the proposed method is discussed in the example of a tensegrity grid.

2 Basic equations

In this section, we present basic equations for tensegrity structures for the completeness of the paper.

2.1 Equilibrium equations

The following properties are assumed for a tensegrity structure:

(1) Members are connected by pin joints.
(2) Topology (connectivity of nodes and members) is specified.
(3) Self-weight is neglected, and no external load exists at the initial self-equilibrium state.
(4) Members are in elastic range, and buckling or yielding is not considered.

From properties (1) and (3), only axial forces exist in the members.

Let m and n^{s} denote the numbers of members and nodes, respectively. If member k is connected by nodes i and j ($i < j$), the kth row of the connectivity matrix $\mathbf{C}^{\mathrm{s}} \in \mathbb{R}^{m \times n^{\mathrm{s}}}$ is defined as

$$\mathbf{C}^{\mathrm{s}}_{(k,p)} = \begin{cases} 1 & (p = i) \\ -1 & (p = j) \\ 0 & (\text{for other cases}) \end{cases} \tag{1}$$

The nodes are classified to n free nodes and n^{f} fixed nodes (supports). Thus, $n^{\mathrm{s}} = n + n^{\mathrm{f}}$. Suppose the nodes are numbered such that the free nodes precede the fixed nodes. Then $\mathbf{C}^{\mathrm{s}}$ is divided to $\mathbf{C} \in \mathbb{R}^{m \times n}$ and $\mathbf{C}^{\mathrm{f}} \in \mathbb{R}^{m \times n^{\mathrm{f}}}$ corresponding to the free and fixed nodes, respectively, as

$$\mathbf{C}^{\mathrm{s}} = (\mathbf{C}, \mathbf{C}^{\mathrm{f}}) \tag{2}$$

Consider a structure in the d-dimensional space, where $d \in \{2, 3\}$. We assume, for brevity, a tensegrity structure in the three-dimensional space for presentation of general formulations. Let $\mathbf{x}$, $\mathbf{y}$, $\mathbf{z}$ ($\in \mathbb{R}^n$) and $\mathbf{x}^{\mathrm{f}}$, $\mathbf{y}^{\mathrm{f}}$, $\mathbf{z}^{\mathrm{f}}$ ($\in \mathbb{R}^{n^{\mathrm{f}}}$) denote the nodal coordinate vectors in x-, y- and z-directions, respectively, of free and fixed nodes. The coordinate difference vectors of the members are denoted by $\mathbf{h}^{\mathrm{x}}$, $\mathbf{h}^{\mathrm{y}}$ and $\mathbf{h}^{\mathrm{z}}$ ($\in \mathbb{R}^m$) for x-, y- and z-directions, respectively, which are calculated from

$$\begin{aligned} \mathbf{h}^{\mathrm{x}} &= \mathbf{C}\mathbf{x} + \mathbf{C}^{\mathrm{f}}\mathbf{x}^{\mathrm{f}} \\ \mathbf{h}^{\mathrm{y}} &= \mathbf{C}\mathbf{y} + \mathbf{C}^{\mathrm{f}}\mathbf{y}^{\mathrm{f}} \\ \mathbf{h}^{\mathrm{z}} &= \mathbf{C}\mathbf{z} + \mathbf{C}^{\mathrm{f}}\mathbf{z}^{\mathrm{f}} \end{aligned} \tag{3}$$

The coordinate difference matrix $\mathbf{H}^{\mathrm{x}}$, $\mathbf{H}^{\mathrm{y}}$ and $\mathbf{H}^{\mathrm{z}}$ ($\in \mathbb{R}^{m \times m}$) are defined as

$$\begin{aligned} \mathbf{H}^{\mathrm{x}} &= \mathrm{diag}(\mathbf{h}^{\mathrm{x}}) \\ \mathbf{H}^{\mathrm{y}} &= \mathrm{diag}(\mathbf{h}^{\mathrm{y}}) \\ \mathbf{H}^{\mathrm{z}} &= \mathrm{diag}(\mathbf{h}^{\mathrm{z}}) \end{aligned} \tag{4}$$

In the following, the components of vectors and matrices are indicated by subscripts, e.g., as $\mathbf{h}^{\mathrm{x}} = (h^{\mathrm{x}}_i)$ and $\mathbf{H}^{\mathrm{x}} = (H^{\mathrm{x}}_{ij})$, respectively. The length matrix $\mathbf{L} = (L_{ij})$ is a diagonal matrix, and its ith diagonal term is given as

$$L_{ii} = \sqrt{(H^{\mathrm{x}}_{ii})^2 + (H^{\mathrm{y}}_{ii})^2 + (H^{\mathrm{z}}_{ii})^2}, \quad (i = 1, \ldots, m) \tag{5}$$

Let $\mathbf{s} \in \mathbb{R}^m$ denote the vector of member forces. In the state of self-equilibrium, the self-equilibrium equation is written as [7]

$$\mathbf{D}\mathbf{s} = \mathbf{0} \tag{6}$$

where the equilibrium matrix $\mathbf{D} \in \mathbb{R}^{3n\times m}$ is defined by

$$\mathbf{D} = \begin{pmatrix} \mathbf{C}^\top \mathbf{H}^{\mathrm{x}} \\ \mathbf{C}^\top \mathbf{H}^{\mathrm{y}} \\ \mathbf{C}^\top \mathbf{H}^{\mathrm{z}} \end{pmatrix} \mathbf{L}^{-1} \tag{7}$$

with $(\,\cdot\,)^\top$ denoting the transpose of a matrix or a vector.

2.2 Self-equilibrium forces

Let r denote the rank of $\mathbf{D}$. Then the equilibrium equation (6) has $q = m-r$ self-equilibrium modes, which are found, as follows, by the singular value decomposition of $\mathbf{D}$.

The non-zero eigenvalues of $\mathbf{D}^\top\mathbf{D}$ are denoted by ω_i $(i = 1,\ldots,r)$. Then the singular value decomposition of $\mathbf{D}$ is written as [8]

$$\mathbf{\Omega} = \mathbf{S}^\top \mathbf{D}\mathbf{R} \tag{8}$$

where

$$\mathbf{\Omega} = \begin{pmatrix} \mathrm{diag}(\omega_1,\ldots,\omega_r) & \mathbf{O} \\ \mathbf{O} & \mathbf{O} \end{pmatrix} \tag{9}$$

with $\mathbf{O}$ being null matrix, and the diagonal terms of $\mathbf{\Omega} \in \mathbb{R}^{3n\times m}$ are called singular values of $\mathbf{D}$. The matrices $\mathbf{R} \in \mathbb{R}^{m\times m}$ and $\mathbf{S} \in \mathbb{R}^{3n\times 3n}$ satisfy the following orthogonality conditions:

$$\begin{aligned} \mathbf{R}^\top\mathbf{R} = \mathbf{R}\mathbf{R}^\top = \mathbf{I}_m \\ \mathbf{S}^\top\mathbf{S} = \mathbf{S}\mathbf{S}^\top = \mathbf{I}_{3n} \end{aligned} \tag{10}$$

where $\mathbf{I}_m \in \mathbb{R}^{m\times m}$ and $\mathbf{I}_n \in \mathbb{R}^{3n\times 3n}$ are the identity matrices.

By premultiplying $\mathbf{S}$ to (8) and using (10), we obtain

$$\mathbf{D}\mathbf{R} = \mathbf{S}\mathbf{\Omega} \tag{11}$$

The column vectors $\mathbf{R}_i$ $(i = r+1, r+2,\ldots,m)$ of $\mathbf{R}$ corresponding to zero singular value satisfy the condition of self-equilibrium force mode as

$$\mathbf{D}\mathbf{R}_i = \mathbf{0} \tag{12}$$

By denoting $\mathbf{g}_i = \mathbf{R}_{i+r}$ $(i = 1,\ldots,q)$, the self-equilibrium force vector $\mathbf{s} \in \mathbb{R}^m$ satisfying $\mathbf{D}\mathbf{s} = \mathbf{0}$ is given as the linear combination of $\mathbf{g}_i$ as

$$\begin{aligned} \mathbf{s} &= \alpha_1\mathbf{g}_1 + \cdots + \alpha_q\mathbf{g}_q \\ &= \mathbf{G}\boldsymbol{\alpha} \end{aligned} \tag{13}$$

where $\boldsymbol{\alpha} = (\alpha_1,\ldots,\alpha_q)^\top$ is the coefficient vector, and $\mathbf{G} = (\mathbf{g}_1,\ldots,\mathbf{g}_q)$ is the matrix of the self-equilibrium forces.

Let $\mathbf{b}_i^\top$ denote the ith row of $\mathbf{G}$. The components of $\mathbf{s}$ are written as

$$s_i = \mathbf{b}_i^\top\boldsymbol{\alpha}, \quad (i = 1,\ldots,m) \tag{14}$$

The self-equilibrium equation with respect to member forces $\mathbf{s}$ in (6) can be rewritten in the following form with respect to the nodal coordinates $\mathbf{x}$, $\mathbf{y}$ and $\mathbf{z}$ [9]:

$$\begin{aligned} \mathbf{E}\mathbf{x} + \mathbf{E}^{\mathrm{f}}\mathbf{x}^{\mathrm{f}} = \mathbf{0} \\ \mathbf{E}\mathbf{y} + \mathbf{E}^{\mathrm{f}}\mathbf{y}^{\mathrm{f}} = \mathbf{0} \\ \mathbf{E}\mathbf{z} + \mathbf{E}^{\mathrm{f}}\mathbf{z}^{\mathrm{f}} = \mathbf{0} \end{aligned} \tag{15}$$

where $\mathbf{E}$ is called force density matrix, and $\mathbf{E}$ and $\mathbf{E}^{\mathrm{f}}$ are given as

$$\begin{aligned} \mathbf{E} &= \mathbf{C}^\top \mathrm{diag}(\mathbf{L}^{-1}\mathbf{s})\mathbf{C} \\ \mathbf{E}^{\mathrm{f}} &= \mathbf{C}^\top \mathrm{diag}(\mathbf{L}^{-1}\mathbf{s})\mathbf{C}^{\mathrm{f}} \end{aligned} \tag{16}$$

2.3 Tangent stiffness matrix and responses to external loads

The tangent stiffness matrix $\mathbf{K}$ for a d-dimensional structure is expressed as the sum of the linear stiffness matrix $\mathbf{K}_{\mathrm{E}}$ and the geometrical stiffness matrix $\mathbf{K}_{\mathrm{G}}$ as [9]

$$\mathbf{K} = \mathbf{K}_{\mathrm{E}} + \mathbf{K}_{\mathrm{G}} \tag{17}$$

where

$$\mathbf{K}_{\mathrm{E}} = \mathbf{D}\bar{\mathbf{K}}\mathbf{D}^{\top}, \quad \mathbf{K}_{\mathrm{G}} = \mathbf{I}_d \otimes \mathbf{E} \tag{18}$$

Here $\mathbf{I}_d \in \mathbb{R}^{d\times d}$ is the identity matrix, and the ith diagonal entry $\bar{K}_{ii}$ of the diagonal matrix $\bar{\mathbf{K}}$ is the stiffness of the ith member; i.e., $\bar{K}_{ii} = A_i E_i / L_{ii}$ where A_i, E_i and L_{ii} are the cross-sectional area, the elastic modulus and the length of member i, respectively.

In the following discussions on stiffness of the structure, the rigid-body motions are assumed to be constrained. Let λ_r ($\lambda_1 \leq \lambda_2 \leq \cdots \leq \lambda_{3n}$) and $\mathbf{\Phi}_r$ denote the rth eigenvalue and eigenvector of $\mathbf{K}$, respectively, which are defined by

$$\mathbf{K}\mathbf{\Phi}_r = \lambda_r \mathbf{\Phi}_r, \quad (r = 1, \ldots, 3n) \tag{19}$$

The eigenvector $\mathbf{\Phi}_r$ is ortho-normalized by

$$\mathbf{\Phi}_r^{\top}\mathbf{\Phi}_s = \delta_{rs}, \quad (r, s = 1, \ldots, 3n) \tag{20}$$

where δ_{rs} is the Kronecker delta. When the external loads applied to a structure are unknown, the best way to strengthen the structure may be to increase its stiffness in the weakest direction. Hence, the lowest eigenvalue $\lambda_{\min}$ ($= \lambda_1$) after constraining the rigid-body motions is maximized as the performance measure in the optimization problem defined in the next section.

Suppose small external loads $\mathbf{P} \in \mathbb{R}^{3n}$ are applied to the structure. The nodal displacements $\mathbf{U} \in \mathbb{R}^{3n}$ are linearly estimated by the tangent stiffness matrix as

$$\mathbf{K}\mathbf{U} = \mathbf{P} \tag{21}$$

In the field of structural optimization, the external work, which is called *compliance* is often used as the performance measure. The compliance W, defined as follows, is to be minimized to obtain the stiffest design against the specified loads:

$$W = \mathbf{U}^{\top}\mathbf{P} \tag{22}$$

3 Optimization problem

Suppose, for brevity, the members $1, \ldots, t$ correspond to the struts, and the members $t+1, \ldots, m$ to cables. The upper bound and lower bound for the forces of the cables and struts, respectively, are denoted by s^{U} (> 0) and s^{L} (< 0). Then the conditions for the member forces are written as

$$s^{\mathrm{L}} \leq s_i \leq 0, \quad (i = 1, \ldots, t) \tag{23a}$$
$$0 \leq s_i \leq s^{\mathrm{U}}, \quad (i = t+1, \ldots, m) \tag{23b}$$

In the process of force design, the geometry (nodal locations) and the topology of the structure are specified. Therefore, the design variables are the coefficients $\boldsymbol{\alpha}$ for the self-equilibrium modes. Note that $\mathbf{K}_{\mathrm{G}}$ depends on $\boldsymbol{\alpha}$, while $\mathbf{K}_{\mathrm{E}}$ is independent of $\boldsymbol{\alpha}$. By using the relation (14), the constraints for the optimization problems are given with respect to $\boldsymbol{\alpha}$ as

$$s^{\mathrm{L}} \leq \mathbf{b}_i^{\top}\boldsymbol{\alpha} \leq 0, \quad (i = 1, \ldots, t) \tag{24a}$$
$$0 \leq \mathbf{b}_i^{\top}\boldsymbol{\alpha} \leq s^{\mathrm{U}}, \quad (i = t+1, \ldots, m) \tag{24b}$$

The lowest eigenvalue $\lambda_{\min}$ after constraining the rigid-body motions is used as the global measure of stiffness and stability of the structure. The optimization problem is formulated as

$$\text{minimize} \quad -\lambda_{\min}(\boldsymbol{\alpha}) \tag{25a}$$
$$\text{subject to} \quad \text{(24a) and (24b)} \tag{25b}$$

The compliance W is next considered as the performance measure representing the stiffness of the structure against the specified external loads $\mathbf{P}$. The optimization

problem is formulated as

$$\begin{aligned} &\text{minimize} \quad W(\boldsymbol{\alpha}) && \text{(26a)}\\ &\text{subject to} \quad \text{(24a) and (24b)} && \text{(26b)} \end{aligned}$$

Note that the numbers of constraints are $2t$ in (24a) and $2(m-t)$ in (24b), because each line of the equations have two inequalities.

The constraints (24a) and (24b) are combined to the following form:

$$H_i(\boldsymbol{\alpha}) \leq 0, \quad (i = 1, \ldots, 2m) \tag{27}$$

The conditions for local optimality of Problem (25) is written as

$$\begin{aligned} &-\frac{\partial \lambda_{\min}}{\partial \alpha_i} + \sum_{j \in \mathcal{A}} \beta_j^{\lambda} \frac{\partial H_j}{\partial \alpha_i} = 0, && \text{(28a)}\\ &\qquad (i = 1, \ldots, q) \\ &\beta_j^{\lambda} \geq 0 \text{ for } (j \in \mathcal{A}^{\lambda}), && \text{(28b)}\\ &\beta_j^{\lambda} = 0 \text{ for } (j \notin \mathcal{A}^{\lambda}) && \text{(28c)} \end{aligned}$$

where β_j^{λ} is the Lagrange multiplier for the jth constraint, and $\mathcal{A}^{\lambda}$ is the set of active constraints. Computation of the gradients (sensitivity coefficients) of the objective functions is presented in Section 4.

The conditions for local optimality of Problem (26) is written as

$$\begin{aligned} &\frac{\partial W}{\partial \alpha_i} + \sum_{j \in \mathcal{A}} \beta_j^{\mathrm{W}} \frac{\partial H_j}{\partial \alpha_i} = 0, && \text{(29a)}\\ &\qquad (i = 1, \ldots, q) \\ &\beta_j^{\mathrm{W}} \geq 0 \text{ for } (j \in \mathcal{A}^{\mathrm{W}}), && \text{(29b)}\\ &\beta_j^{\mathrm{W}} = 0 \text{ for } (j \notin \mathcal{A}^{\mathrm{W}}) && \text{(29c)} \end{aligned}$$

where β_j^{W} is the Lagrange multiplier for the jth constraint, and $\mathcal{A}^{\mathrm{W}}$ is the set of active constraints.

Finally, we consider the problem of simultaneously minimizing the two objective functions $-\lambda_{\min}(\boldsymbol{\alpha})$ and $W(\boldsymbol{\alpha})$. This problem is formulated as a multiobjective programming problem as

$$\begin{aligned} &\text{minimize} \quad -\lambda_{\min}(\boldsymbol{\alpha}),\ W(\boldsymbol{\alpha}) && \text{(30a)}\\ &\text{subject to} \quad \text{(24a) and (24b)} && \text{(30b)} \end{aligned}$$

Since it is not generally possible to find an optimal solution that minimizes the two objectives simultaneously, a compromise solution is selected as a solution to a multiobjective optimization problem. A feasible solution satisfying all the constraints is called Pareto optimal solution, if there exists no feasible solution in its neighborhood that simultaneously improves the two objective functions [10].

If we assume the monotonicity of the objective functions $-\lambda_{\min}(\alpha)$ and $W(\alpha)$ with respect to $\boldsymbol{\alpha}$, we can generate a set of Pareto optimal solutions by enumeration of vertices of the convex feasible region of $\boldsymbol{\alpha}$ defined by (24) [11,12].

A Pareto optimal solution is characterized as an optimal solution of the weighted sum of the objective functions. Let c^{λ} (> 0) and c^{W} (> 0) denote the weight coefficients for the two objective functions $-\lambda_{\min}(\boldsymbol{\alpha})$ and $W(\boldsymbol{\alpha})$, respectively. The set of the active constraints at a vertex of the feasible region is denoted by $\mathcal{A}$. If there exists a set of Lagrange multipliers $\beta_1, \ldots, \beta_{2m}$ satisfying the following conditions, then the vertex represents a Pareto optimal solution:

$$\begin{aligned} &-c^{\lambda}\frac{\partial \lambda_{\min}}{\partial \alpha_i} + c^{\mathrm{W}}\frac{\partial W}{\partial \alpha_i} && \text{(31a)}\\ &\qquad + \sum_{j \in \mathcal{A}} \beta_j \frac{\partial H_j}{\partial \alpha_i} = 0, \quad (i = 1, \ldots, q) \\ &\beta_j \geq 0 \text{ for } (j \in \mathcal{A}), && \text{(31b)}\\ &\beta_j = 0 \text{ for } (j \notin \mathcal{A}) && \text{(31c)} \end{aligned}$$

The algorithm of force design by vertex enumeration of the feasible region is summarized as follows:

Step 1 Specify the geometry, topology and material property of the structure.

Step 2 Construct the equilibrium matrix $\mathbf{D}$ from (7), and compute the self-equilibrium modes $\mathbf{g}_1, \ldots, \mathbf{g}_q$ by the singular value decomposition (11).

Step 3 Assign the bound constraints (24) for the axial forces.

Step 4 Generate the list of vertices of the feasible region of the coefficients $\boldsymbol{\alpha}$.

Step 5 Assign the support conditions and the external loads.

Step 6 Compute the tangent stiffness matrix $\mathbf{K}$ from (17) at each vertex.

Step 6 Compute the lowest eigenvalue $\lambda_{\min}$ from (19) and the compliance W from (21) and (22).

Step 7 Compute the sensitivity coefficients of $\lambda_{\min}$ and W with respect to α_i.

Step 8 Evaluate the property of the vertex based on the optimality conditions.

4 Sensitivity analysis

In this section, formulations of sensitivity analysis are presented to compute the gradients of the static responses and the eigenvalues of the tangent stiffness matrix.

Differentiation of (19) and (20) with respect to the design variable α_i leads to

$$\frac{\partial \mathbf{K}}{\partial \alpha_i}\boldsymbol{\Phi}_r + \mathbf{K}\frac{\partial \boldsymbol{\Phi}_r}{\partial \alpha_i} = \frac{\partial \lambda_r}{\partial \alpha_i} + \lambda_r \frac{\partial \boldsymbol{\Phi}_r}{\partial \alpha_i} \tag{32}$$

$$2\boldsymbol{\Phi}_r^\top \frac{\partial \boldsymbol{\Phi}_r}{\partial \alpha_i} = 0 \tag{33}$$

By premultiplying $\boldsymbol{\Phi}_r^\top$ to both sides of (32) and using (19) and (20), we obtain

$$\frac{\partial \lambda_r}{\partial \alpha_i} = \boldsymbol{\Phi}_r^\top \frac{\partial \mathbf{K}}{\partial \alpha_i}\boldsymbol{\Phi}_r \tag{34}$$

Incorporation of (17) into (34) leads to

$$\frac{\partial \lambda_r}{\partial \alpha_i} = \boldsymbol{\Phi}_r^\top \frac{\partial (\mathbf{K}_{\mathrm{E}} + \mathbf{K}_{\mathrm{G}})}{\partial \alpha_i}\boldsymbol{\Phi}_r \tag{35}$$

Since $\mathbf{K}_{\mathrm{E}}$ is independent of α_i, we obtain

$$\frac{\partial \lambda_r}{\partial \alpha_i} = \boldsymbol{\Phi}_r^\top \frac{\partial \mathbf{K}_{\mathrm{G}}}{\partial \alpha_i}\boldsymbol{\Phi}_r \tag{36}$$

From (13), (16) and (18), the following relation is derived:

$$\frac{\partial \mathbf{K}_{\mathrm{G}}}{\partial \alpha_i} = \mathbf{C}^\top \operatorname{diag}(\mathbf{L}^{-1}\mathbf{g}_i)\mathbf{C} \tag{37}$$

From (21) and (22), the external work W depends on $\boldsymbol{\alpha}$ explicitly through $\mathbf{K}(\boldsymbol{\alpha})$ and implicitly through $\mathbf{U}(\boldsymbol{\alpha})$. Therefore, W is reformulated as

$$\begin{aligned} W &= \mathbf{U}^\top(\boldsymbol{\alpha})\mathbf{P} \\ &= \mathbf{U}^\top(\boldsymbol{\alpha})\mathbf{K}(\boldsymbol{\alpha})\mathbf{U}(\boldsymbol{\alpha}) \\ &= 2\Big(\mathbf{U}^\top(\boldsymbol{\alpha})\mathbf{P} - \frac{1}{2}\mathbf{U}^\top(\boldsymbol{\alpha})\mathbf{K}(\boldsymbol{\alpha})\mathbf{U}(\boldsymbol{\alpha})\Big) \end{aligned} \tag{38}$$

and the sensitivity coefficient of W with respect to α_i is obtained as

$$\begin{aligned} \frac{\partial W}{\partial \alpha_i} &= -\mathbf{U}^\top \frac{\partial \mathbf{K}}{\partial \alpha_i}\mathbf{U} + 2(\mathbf{P} - \mathbf{K}\mathbf{U})^\top \frac{\partial \mathbf{U}}{\partial \alpha_i} \\ &= -\mathbf{U}^\top \frac{\partial \mathbf{K}}{\partial \alpha_i}\mathbf{U} \\ &= -\mathbf{U}^\top \frac{\partial \mathbf{K}_{\mathrm{G}}}{\partial \alpha_i}\mathbf{U} \end{aligned} \tag{39}$$

where (17) and (21) have been used.

Since $\mathbf{K}_{\mathrm{G}}$ is a linear function of $\boldsymbol{\alpha}$, $\partial \mathbf{K}_{\mathrm{G}}/\partial \alpha_i$ is a constant matrix as seen in (37). Therefore, if $\boldsymbol{\Phi}_{\min}$ corresponding to $\lambda_{\min}$ and $\mathbf{U}$ are almost constant in the feasible region, then $\lambda_{\min}$ and W are monotonic functions of $\boldsymbol{\alpha}$.

5 Numerical examples

The tensegrity grid as shown in Fig. 1 is used as the example structure [13]. The structure is constructed by consecutively assembling the unit cell as shown in Fig. 2

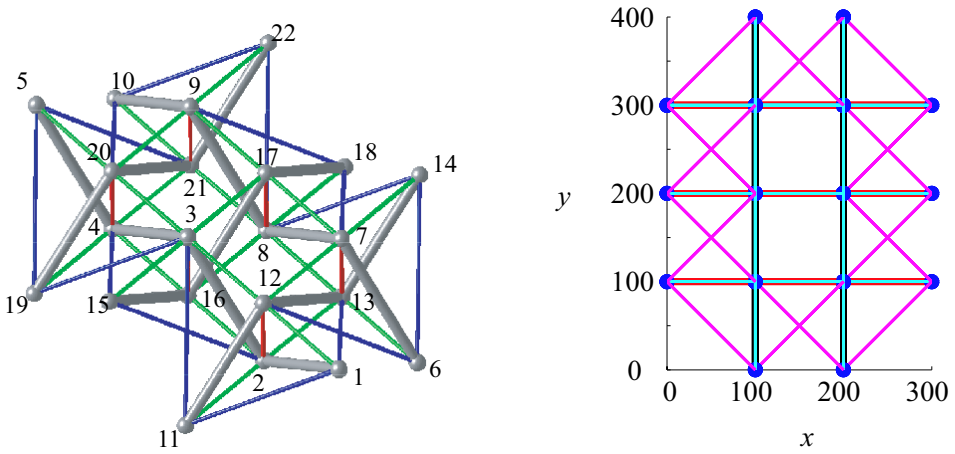

(a) diagonal view (b) plan view

Fig. 1. Tensegrity grid constructed by assembling the unit cell shown in Fig. 2 in x- and y-directions. This example structure consists of three rows and two columns of struts.

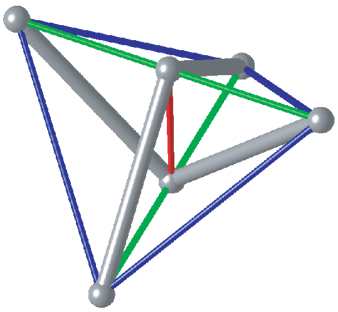

Fig. 2. Unit cell for the tensegrity grid.

in x- and y-directions. The thick and thin lines in the figures are struts and cables (or bars), respectively. Note that the members in thin lines that are connected to the boundary nodes do not carry any prestress at the self-equilibrium state; these members are called bars and assumed to have stiffness in both of compression and tension in the structural analysis.

Let r and c denote the numbers of rows (parallel to x-axis) and columns (parallel to y-axis) of the struts, respectively; i.e., there exist $r+1$ struts in each column and $c+1$ struts in each row. Therefore, the structure has $2rc+r+c$ struts and $n = 2(rc+r+c)$ nodes, and the total number of members is $m = 7rc + 5r + 5c - 4$. The rank deficiency of the linear stiffness matrix $\mathbf{K}_{\mathrm{E}}$ after constraining the six rigid-body motions is equal to 1; i.e., this structures has only one infinitesimal mechanism.

The structure in Fig. 1 studied in the numerical examples has three and four struts in x- and y-directions, respectively; i.e., $r = 3$ and $c = 2$. Hence, there are $m = 63$ members and $n = 22$ nodes in total. The x- and y-coordinates (mm) of the nodes are shown in the plan view of the structure in Fig. 1(b), and the height of the grid is 100 mm.

The elastic modulus of all members is $E = 20 \times 10^3$ N/mm^2. The cross-sectional

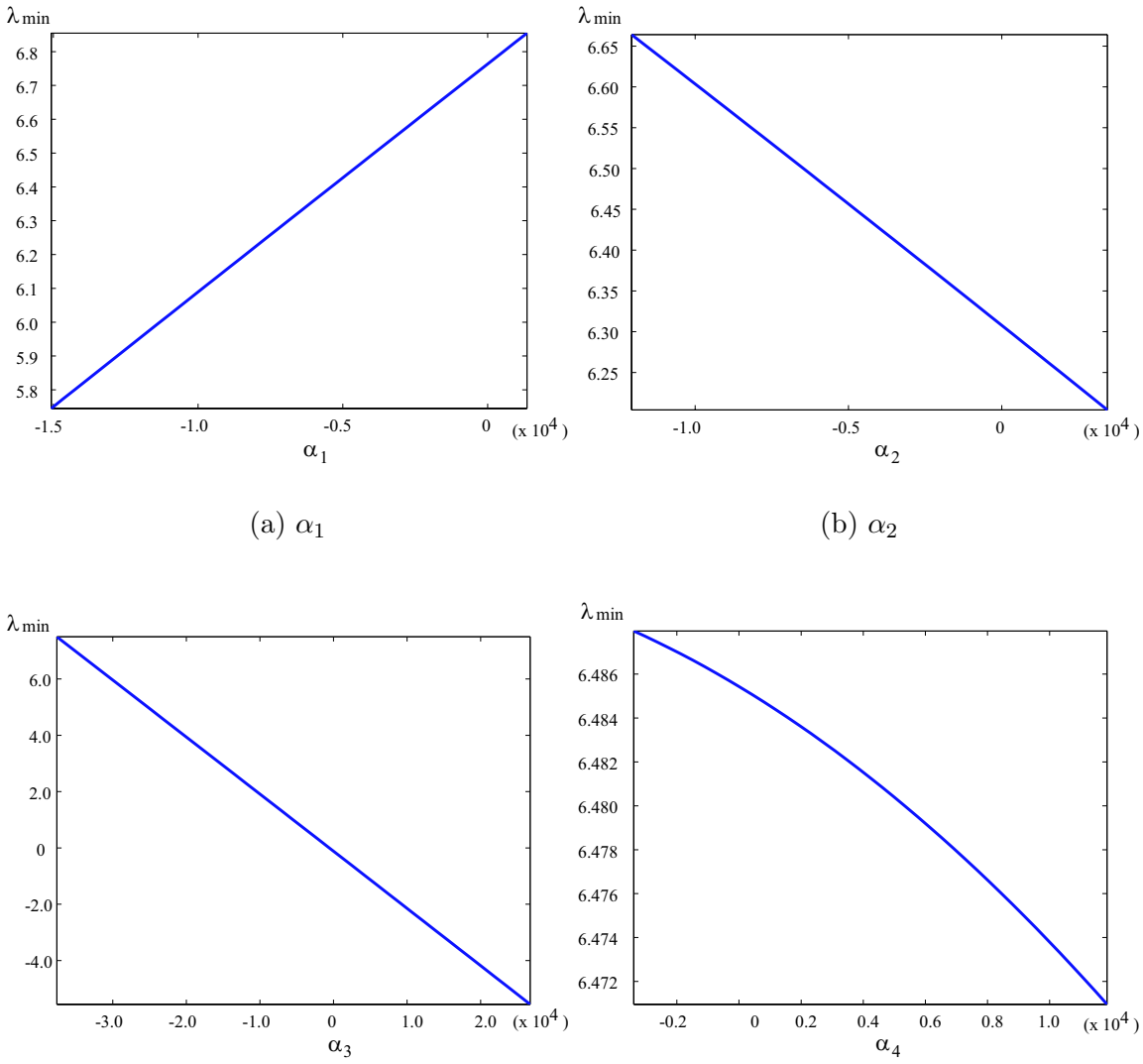

(a) α_1 (b) α_2

(c) α_3 (d) α_4

Fig. 3. Variation of $\lambda_{\min}$ with respect to $\boldsymbol{\alpha} = (\alpha_1, \ldots, \alpha_4)^\top$ in the feasible region.

areas are 50 mm^2 for struts and bars, and 5 mm^2 for cables. In the following, the units of length and force are mm and N, respectively.

The lower bound s^{L} and the upper bound s^{U} for the axial forces of the struts and cables, respectively, are -1000 N and 1000 N; equivalently, the maximum absolute values of the strains are 0.1% for the struts and 1% for the cables.

The rank of the equilibrium matrix $\mathbf{D}$ is $r = 59$. Therefore, the structure has four ($q = 63 - 59 = 4$) force modes at the self-equilibrium state, which are denoted by $\mathbf{g}_1, \ldots, \mathbf{g}_4$ with the coefficients $\boldsymbol{\alpha} = (\alpha_1, \ldots, \alpha_4)^\top$.

We use a software cdd+ [14] for enumeration of vertices of the feasible region defined by linear equality and inequality constraints. In this example, there exist 74 vertices of the feasible region for the coefficients $\boldsymbol{\alpha}$ of the member forces. The min-

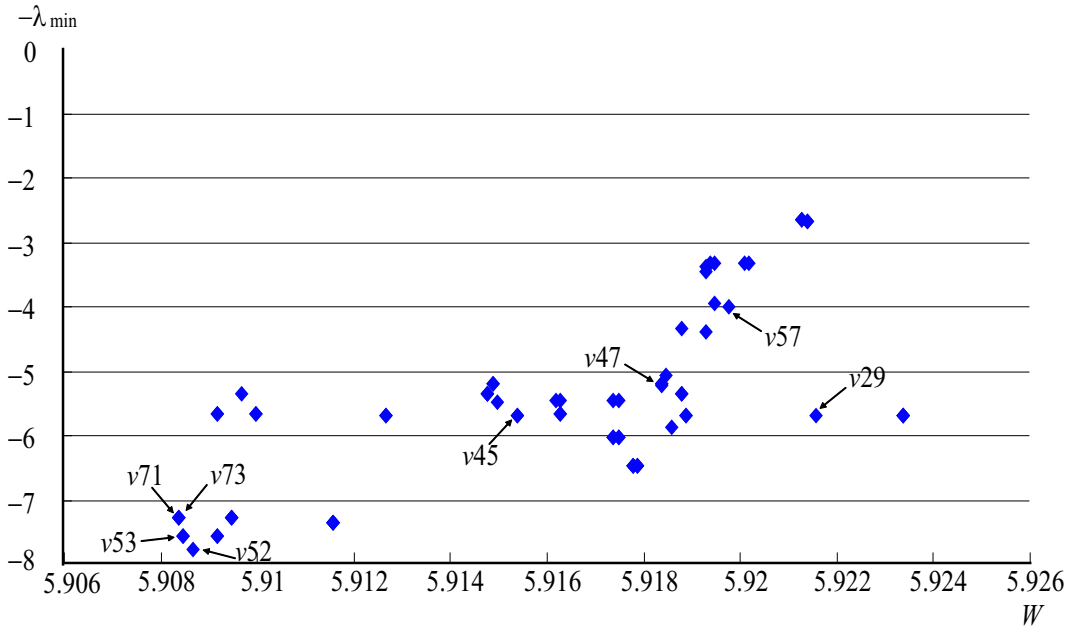

Fig. 4. Minimum eigenvalue $\lambda_{\min}$ and compliance W at the vertices of the feasible region found by cdd+.

Table 1
Minimum eigenvalue $\lambda_{\min}$ and compliance W at the selected vertices of the feasible region.

Vertex	$v29$	$v45$	$v47$	$v52$	$v53$	$v57$	$v71$	$v72$	$v73$
$\lambda_{\min}$	0.56764	0.56724	0.51779	0.77422	0.75590	0.39945	0.72640	0.56684	0.72634
W	5.9216	5.9154	5.9184	5.9087	5.9085	5.9198	5.9084	5.9127	5.9084
$\boldsymbol{\beta}^{\lambda}$	58.373	0.9183	3.7167	0.7372	−2.4937	1.8461	3.2041	−0.0025	3.2037
	−35.233	−0.9449	−1.3498	0.7409	0.4044	5.6979	1.2345	−2.8025	3.1873
	−0.4622	−5.2854	−0.9318	1.0550	2.0705	−25990	1.9538	1.3107	−2.0713
	−0.4622	2.6552	−0.9318	1.0591	3.5252	4591.7	−3.0242	1.3168	−0.9517
	2.634		−1.3192			4591.7			
$\boldsymbol{\beta}^{\mathrm{W}}$	−163340	33.549	10.815	18.012	12.808	20.644	5.5460	−25.766	5.5440
	94304	9.3980	−19.175	17.789	19.733	−20.103	18.674	−26.954	29.893
	−26.280	−67.449	−13.808	−5.5720	10.976	−105410	11.225	19.884	−11.900
	−26.280	−15.229	−13.808	8.3140	−4, 5100	1.8620	37.490	37.889	15.655
	17.916		11.998			18620			

imum eigenvalue $\lambda_{\min}$ of $\mathbf{K}$ is positive at all the vertices after constraining the rigid-body motions. The variations of $\lambda_{\min}$ in feasible region are illustrated in Fig. 3, where one of the variables $\alpha_1, \ldots, \alpha_4$ is varied in each figure starting from the center of the feasible region.

The value of $\lambda_{\min}$ at the center is 0.04812, and the quadratic forms $\boldsymbol{\Phi}_{\min}^{\top}\mathbf{K}_{\mathrm{E}}\boldsymbol{\Phi}_{\min}$ and $\boldsymbol{\Phi}_{\min}^{\top}\mathbf{K}_{\mathrm{G}}\boldsymbol{\Phi}_{\min}$ are 0.00163 and 0.64649, respectively; i.e., contribution of the linear stiffness is much smaller than that of the geometrical stiffness, because $\boldsymbol{\Phi}_{\min}$ is close to the direction of the infinitesimal mechanism of the structure. This indicates the great influence of the prestress on stiffness of the structure, and shows the importance of force design for a structure with desired stiffness. Furthermore, as is seen from Fig. 3, $\lambda_{\min}$ is an approximately linear and

Table 2
Active constraints for forces at vertices $v52$, $v53$ and $v71$; '+': $s_i = 1000$ N, '−': $s_i = -1000$ N, 0: $s_i = 0$.

Member (node 1:node 2)	7:8	8:9	12:13	20:21	3:16	7:13	8:17	9:21
$v52$			−	−	+		+	
$v53$	−	−	−	−			+	
$v71$	−	−	−	−		+		+

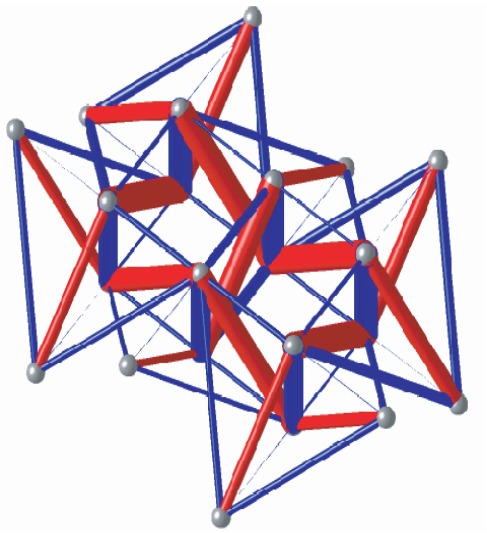

Fig. 5. Member forces at v71; red: compression, blue: tension.

monotonic function of $\boldsymbol{\alpha}$.

The compliance W under static loads is next investigated. The vertical loads 10 N are given asymmetrically in the negative direction of z-axis at nodes 3, 12 and 20 indicated in Fig. 1(a). To exclude the rigid-body motions of the structure, the displacements are constrained at nodes 11 and 19 in x-direction, at nodes 6 and 11 in y-direction, and at nodes 6, 10, 11, 18 and 19 in z-direction. Note again that the loads are assumed to be sufficiently small to investigate the stiffness against small disturbance by linear analysis. It has been confirmed that the compliance is also a monotonic function of $\boldsymbol{\alpha}$ in the feasible region.

The values of $\lambda_{\min}$ and W at the selected vertices of the feasible region are listed in Table 1 and plotted in Fig. 4. The coefficients β_j^{λ} and β_j^{W} for expanding the gradients of $\lambda_{\min}$ and W, respectively, by the gradients of the active constraints as in (28) and (29) are also listed. Note that the active constraints are degenerate (redundant) due to symmetry, if the number of active constraints is greater than four. For example, the vertex $v29$ has five active constraints, and the third and fourth constraints are degenerate. As can be seen from Table 1 and Fig. 4, $-\lambda_{\min}$ is minimized ($\lambda_{\min}$ is maximized) at vertex $v52$, and W is minimized at vertex $v71$. They are the optimal solutions for the two single objective functions, respectively.

It is confirmed in Table 1 that all the coefficients β_j^{λ} and β_j^{W} are positive at $v52$ and $v71$, respectively. Moreover, the vertex $v53$ is a Pareto optimal solution. This can be verified from Table 1 that the condition $\beta_j \geq 0$ in (31) for the active constraints is satisfied for $1.9570 \leq c^{\mathrm{W}}/c^{\lambda} \leq 7.8164$. It is

also seen from Fig. 4 that there is no vertex that improves the two objectives simultaneously from $v53$.

The active force constraints are listed in Table 2 for vertices $v52$, $v53$ and $v71$, where each member is indicated by the node numbers at both ends shown in Fig. 1. '+' denotes a cable with tensile force equal to the upper bound, and '−' denotes a strut with compressive force equal to the lower bound. The member forces at $v71$ are plotted in Fig. 5, where the width of each member is proportional to the absolute value of its force, and the red and blue members are in compressive and tensile states, respectively.

6 Conclusions.

A force design method has been presented for tensegrity structures by enumeration of the vertices of feasible region of the prestresses in self-equilibrium state. Constraints are given for member forces so that the unilateral properties of the stresses in cables and struts are satisfied.

A multiobjective optimization problem is formulated to simultaneously maximize the lowest eigenvalue of the tangent stiffness matrix and minimize the compliance (external work) against a specified set of external loads. The conditions for Pareto optimal solutions have been explicitly derived by using the gradients of the objective functions and the constraints.

In the numerical examples, the monotonicity of the objective functions is investigated for a tensegrity structure that has only one infinitesimal mechanism. Pareto optimal solutions have been found by enumerating the vertices of the feasible region.

Although a simple case with only two objective functions has been investigated in this paper, the proposed method is very effective for the case where many performance measures satisfying monotonicity property are to be investigated in the force design of tensegrity structures.

REFERENCES

[1] R. Motro, 1992. Tensegrity systems: the state of the art. Int. J. Space Structures. Vol. 7, No. 2, pp. 75–83.

[2] H. Lalvani, 1996. Origins of tensegrity: views of Emmerich, Fuller and Snelson, Int. J. Space Structures, Vol.11, No. 1 & 2, pp. 27–55.

[3] R. Connelly, 1999. Tensegrity Structures: Why are they Stable? Rigidity Theory and Applications, edited by Thorpe and Duxbury, Kluwer/Plenum Publishers, pp. 47–54.

[4] A. G. Tibert and S. Pellegrino, 2003. Review of form-finding methods for tensegrity structures, Int. J. Space Structures, Vol.18, No.4, pp. 209–223.

[5] J. Y. Zhang and M. Ohsaki, 2007. Optimization methods for force and shape design of tensegrity structures, Proc. 7th World Congress on Structural and Multidisciplinary Optimization, Seoul, Korea.

[6] M. Ohsaki and J. Y. Zhang, 2006. Stability conditions of prestressed pin-jointed structures, Int. J. Non-Linear Mechanics, Vol. 41, pp. 1109–1117.

[7] H. J. Schek , 1974. The force density method for form finding and computation of general networks, Comp. Meth. Appl. Mech. Engng., Vol. 3, pp. 115–134.

[8] R. A. Horn and C.R. Johnson, 1990. Matrix Analysis. Cambridge University Press (Reprint edition).

[9] J. Y. Zhang and M. Ohsaki, 2006. Adaptive force density method for form-finding problem of tensegrity

structures. Int. J. Solids Struct., Vol. 43, pp. 5658–5673.

[10] J. L. Cohon, 1978. Multiobjective Programming and Planning, Vol. 140, Mathematics in Science and Engineering, Academic Press.

[11] D. Avis and K. Fukuda, 1992. A pivoting algorithm for convex hulls and vertex enumeration of arrangements and polyhedra, Discrete Comput. Geom., Vol. 8, pp. 295–313.

[12] D. Avis and K. Fukuda, 1996. Reverse search for enumeration. Discrete Applied Math., Vol. 65(1–3), pp. 21–46.

[13] R. Motro, 2003. Tensegrity Structural Systems for the Future, Butterworth-Heinemann.

[14] K. Fukuda, 1999. cdd+ Ver. 0.76 User's Manual, Inst. Operation Res., ETH-Zentrum, Zurich, Switzerland.